Synthesis and biological evaluation of 3-styrylchromone derivatives as selective monoamine oxidase B inhibitors.

Koichi Takao[1], Yuri Takemura[1], Junko Nagai[2], Hitoshi Kamauchi[1], Kaori Hoshi[1], Ryo Mabashi[1], Yoshihiro Uesawa[2] and Yoshiaki Sugita[1]

1 Laboratory of Bioorganic Chemistry, Department of Pharmaceutical Sciences, Faculty of Pharmacy and Pharmaceutical Sciences, Josai University; 1-1 Keyaki-dai, Sakado, Saitama 350-0295, Japan
2 Department of Medical Molecular Informatics, Meiji Pharmaceutical University, 2-522-1 Noshio, Kiyose, Tokyo 204-8588, Japan.

Abstract

A series of 3-styrylchromone derivatives was synthesized and evaluated for monoamine oxidase (MAO) A and B inhibitory activities. Most of all derivatives inhibited MAO-B selectively, except compound **21**. Compound **19**, which had a methoxy group at R^2 on the chromone ring and chlorine at R^4 on phenyl ring, potently inhibited MAO-B, with an IC_{50} value of 2.2 nM. Compound **1** showed the highest MAO-B selectivity, with a selectivity index of >3700. Further analysis of these compounds indicated that compounds **1** and **19** were reversible and mixed-type MAO-B inhibitors, suggesting that their mode of action may be through tight-binding inhibition to MAO-B.

Quantitative structure–activity relationship (QSAR) analyses of the 3-styrylchromone derivatives were conducted using their pIC_{50} values, through Molecular Operating Environment (MOE) and Dragon. There were 1,796 descriptors of MAO-B inhibitory activity, which showed significant correlations ($P < 0.05$). Further investigation of the 3-styrylchromone structures as useful scaffolds was performed through three-dimensional-QSAR studies using AutoGPA, which is based on the molecular field analysis algorithm using MOE. The MAO-B inhibitory activity model constructed using pIC_{50} value index exhibited a determination coefficients (R^2) of 0.972 and a Leave-One-Out cross-validated determination coefficients (Q^2) of 0.914.

These data suggest that the 3-styrylchromone derivatives assessed herein may be suitable for the design and development of novel MAO inhibitors.

Keywords

3-Styrylchromone; Monoamine oxidase-A; Monoamine oxidase-B; Quantitative

structure–activity relationship QSAR; Molecular Operating Environment MOE; AuroGPA

Introduction

Monoamine oxidase (MAO, EC 1.4.3.4), a flavin adenine dinucleotide (FAD) enzyme, catalyzes the oxidative deamination of monoamine neurotransmitters. MAO has two isoforms, MAO-A and MAO-B. MAO-A preferentially degrades epinephrine, norepinephrine and serotonin, and is inhibited irreversibly by clorgyline, while MAO-B preferentially degrades dopamine, β-phenethylamine and benzylamine, and is inhibited irreversibly by (*R*)-(-)-deprenyl. Studies on MAO inhibitors have mostly been based on the metabolism of these important neurotransmitter targets [1-3].

Chromone (4*H*-1-benzopyran-4-one) derivatives are widely distributed in natural product, such as flavones, isoflavones and 2-styrylchromones, and form an important class of oxygenated heterocyclic compounds in drug discovery [4-6]. Based on reports of MAO inhibition by synthetic chromone derivatives, we synthesized a series of new chromone derivatives such as 2-azolylchromone [7], 3-styrylchromene [8], and 2-styrylchromone [9], and tested their MAO inhibitory activity. Recently, we reported on the syntheses and MAO inhibitory activities of 2-cyclicaminochromone derivatives and 3-cyclicaminochromone derivatives [10]. The 3-cyclicaminochromone derivatives inhibited MAO-B more potently than the 2-cyclicaminochromone derivatives. These results led us to investigate the MAO-B inhibitory activity of 3-styrylchromone derivatives, including those of the newly synthesized compounds. The present report deals with the synthesis of a series of 3-styrylchromone derivatives (Chart 1), their inhibitory activities against human MAO-A and MAO-B, and the quantitative structure–activity relationship (QSAR) of the derivatives to MAO-A and MAO-B.

Results and discussion

Chemistry

Synthesis of 3-styrylchromone derivatives

3-Styrylchromone derivatives (**1**-**24**) were synthesized according to previously reported method, with minor modifications [11]. 3-Formylchromone derivatives (**IIa-c**) were reacted with selected phenylacetic acid or phenylmalonic acid derivatives by Knoevenagel condensation. 3-Styrylchromones having a hydroxy group (**5**, **13**, **21**) were synthesized by condensation of 3-formylchromone derivatives and protected 4-hydroxyphenylacetic acids (**IIIi**, **IIIj**) followed by removal the protecting group.

In all cases, satisfactory yields were obtained. The 3-formylchromone derivatives (**IIa-c**) were synthesized from 2-hydroxyacetophenone derivatives (**Ia-c**) using the Vilsmeier-Haack reagent. We used previously reported conditions to synthesize 7-methoxy-3-formylchromone at very low yields (approximately 0–5%). We chose to use the method of Yan *et al*. [12], which showd that the difluorodioxaborin of 2-hydroxy-4-methoxyacetophenone increased 7-methoxy-3-formylchromone yield (Chart 1).

Chart 1

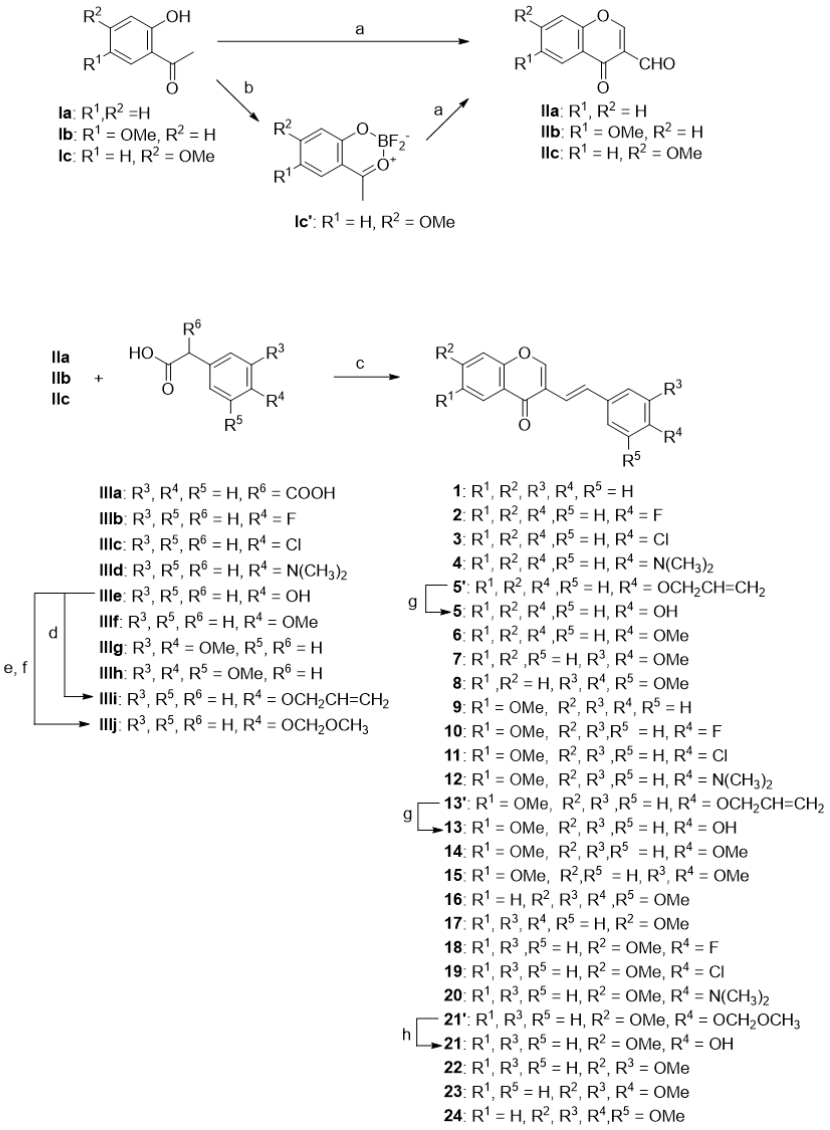

Biological activity

All the synthesized 3-styrylchromone derivatives (compounds **1** to **24**) were evaluated for MAO-A and MAO-B inhibitory activities (Table 1). Effects of the substituent of the chromone ring (R^1, R^2) and the phenyl ring (R^3, R^4, R^5) on MAO inhibitory activity revealed some structure-activity relationships.

Table 1

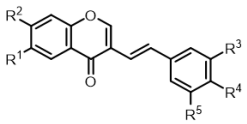

Compound	R^1	R^2	R^3	R^4	R^5	MAO-A IC_{50} (μM)	MAO-B IC_{50} (μM)	S. I.
1	H	H	H	H	H	>100	0.027 ± 0.0030	>3700
2	H	H	H	F	H	0.62 ± 0.044	0.0086 ± 0.00043	72
3	H	H	H	Cl	H	0.39 ± 0.096	0.0059 ± 0.00032	66
4	H	H	H	$N(CH_3)_2$	H	42 ± 3.9	0.048 ± 0.0046	875
5	H	H	H	OH	H	2.6 ± 0.15	0.037 ± 0.0029	70
6	H	H	H	OMe	H	>100	0.029 ± 0.0016	>3400
7	H	H	OMe	OMe	H	33 ± 5.5	0.16 ± 0.021	206
8	H	H	OMe	OMe	OMe	67 ± 3.6	0.23 ± 0.031	291
9	OMe	H	H	H	H	2.5 ± 0.43	0.075 ± 0.0045	33
10	OMe	H	H	F	H	0.38 ± 0.034	0.034 ± 0.0023	11
11	OMe	H	H	Cl	H	4.1 ± 0.15	0.028 ± 0.0030	146
12	OMe	H	H	$N(CH_3)_2$	H	59 ± 1.6	0.23 ± 0.011	257
13	OMe	H	H	OH	H	8.7 ± 0.87	0.33 ± 0.026	26
14	OMe	H	H	OMe	H	35 ± 3.3	0.15 ± 0.011	233
15	OMe	H	OMe	OMe	H	61 ± 7.3	0.80 ± 0.040	76
16	OMe	H	OMe	OMe	OMe	>100	2.5 ± 0.41	>40
17	H	OMe	H	H	H	0.12 ± 0.0083	0.016 ± 0.0019	8
18	H	OMe	H	F	H	0.041 ± 0.0018	0.0031 ± 0.00029	13
19	H	OMe	H	Cl	H	0.025 ± 0.0013	0.0022 ± 0.000074	11
20	H	OMe	H	$N(CH_3)_2$	H	0.49 ± 0.093	0.0061 ± 0.00032	80
21	H	OMe	H	OH	H	0.022 ± 0.0014	0.047 ± 0.0031	-
22	H	OMe	H	OMe	H	0.069 ± 0.0031	0.0068 ± 0.00037	10
23	H	OMe	OMe	OMe	H	19 ± 1.1	0.033 ± 0.0024	576
24	H	OMe	OMe	OMe	OMe	7.3 ± 0.60	0.021 ± 0.0036	348
Prgyline						4.6 ± 0.27	0.22 ± 0.024	21
Clorgyline						0.0049 ± 0.00028	5.8 ± 0.34	0.00085
Safinamide						100	0.05 ± 0.063	2000

Inhibitory activities of 3-styrylchromone derivatives towards MAO-A and MAO-B

Among the 3-styrylchromone derivatives, compounds **2**, **3**, **10**, **17** and **20** showed IC_{50} values against MAO-A of less than 1 μM, and compounds **18**, **19**, **21** and **22** showed IC_{50} values against MAO-A of less than 0.1 μM, suggesting that the introduction of a substituent on R^2 and/or R^4 was effective for MAO-A inhibition. Compounds **19** and **21** showed significant MAO-A inhibitory activities with IC_{50} values of 25 and 22 nM, respectively, while clorgyline used as a positive control, showed IC_{50} of 4.9 nM.

All evaluated 3-styrylchromone derivatives, except compound **21**, showed very low IC_{50} values for MAO-B compared to their respective IC_{50} values for MAO-A. In particular, compound **18** and **19** showed significantly lower IC_{50} values for MAO-B of 3.1 or 2.2 nM, respectively, while safinamide, used as a positive control, showed an IC_{50} of 50 nM. This suggested the usefulness of introducing a substituent on R^2 and R^4 for the inhibition of MAO.

The selectivity index (SI) was expressed as the ratio of IC_{50} value of MAO-A to that for MAO-B for each compound. Most of derivatives, except for compound **21**, showed

SI values higher than 5; particularly, compounds **1** and **6** showed SIs of >3400, and safinamide showed an SI of 2000. The following description was narrowed to MAO-B.

Substituent effect of 3-styrylchromone on MAO-B inhibition

The presence of methoxy groups at R^1, R^2 or R^3 caused a statistically significant inhibition of MAO-B ($p<0.05$), as summarized in Fig. 1. The pIC_{50} values of the derivatives with methoxy groups at R^1, R^2, or R^3 were compared with those of derivatives with hydrogen. The results clearly showed that methoxy groups at R^1 or R^3 reduced MAO-B inhibitory activity, and that a methoxy group at R^2 increased this activity. In addition, a substituent at R^4 was generally thought to increase the MAO-B inhibitory activity, as the chloride at R^4 increased MAO-B inhibitory activity. Substituent at R^5 (compound **8**, **16**, and **24**) seemed to weaken the inhibitory activity. Takao *et al*. recently reported that chlorine substitution on the phenyl rings of 2-styrylchromone and 3-styrylchromene potentiated their MAO-B inhibitory activities [8,9].

Fig. 1A

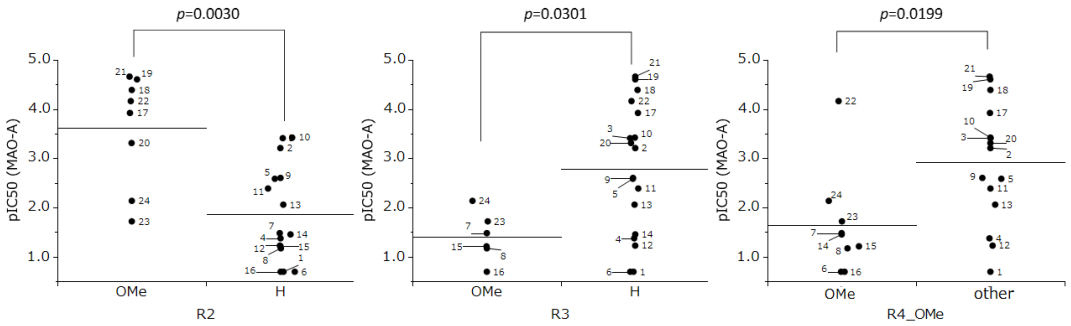

Fig. 1B

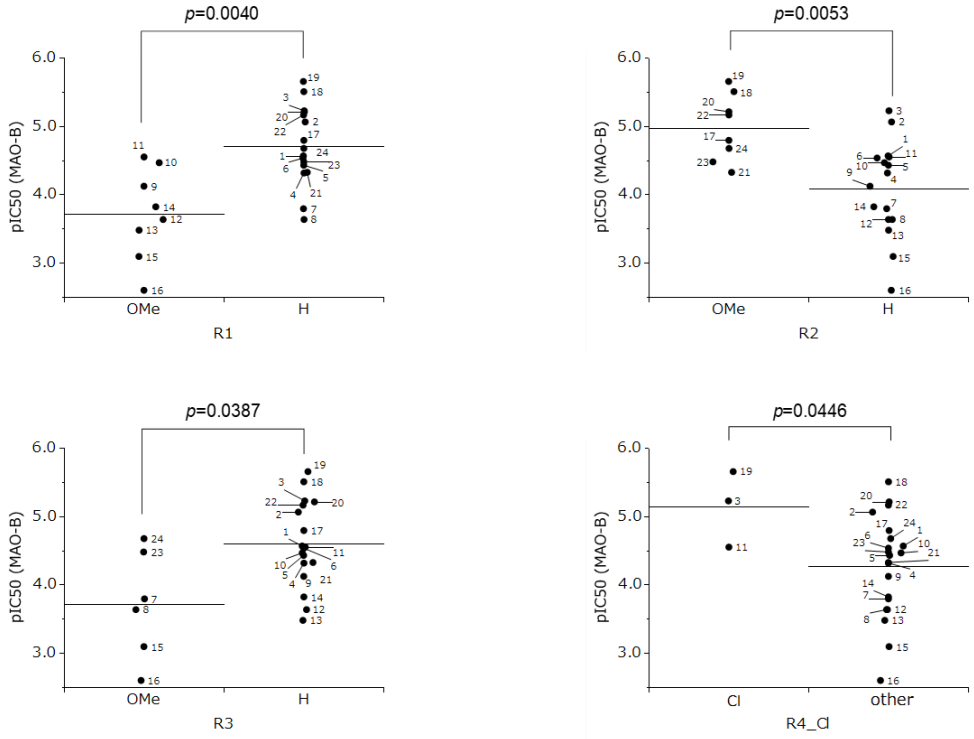

Kinetic studies of compounds **1** and **19**

Compound **1**, the most selective MAO-B inhibitor, and compound **19**, the most potent MAO-B inhibitor, were chosen for the following kinetic studies (Fig. 2). The lines of the Lineweaver-Burk plots for these two compounds did not intersect on the y-axis, suggesting that the mode of MAO-B inhibition by 3-styrylchromone derivatives may be a mixed-type, such that the derivatives act as a tight-binding inhibitor, as indicated in previous reports [13]. Th apparent Ki value was 18 nM for compound **1** and 1.5 nM for compound **19**.

Fig. 2A

Compound 1

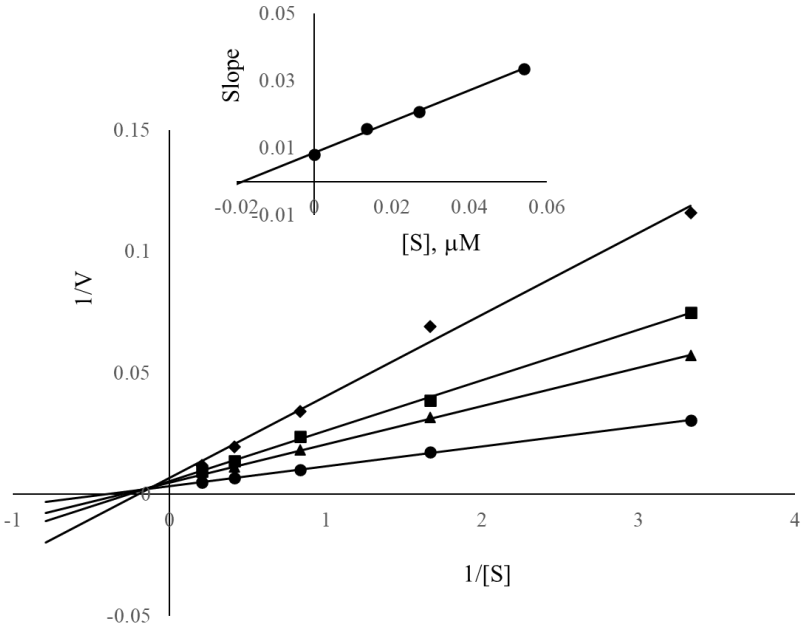

Fig. 2B

Compound 19

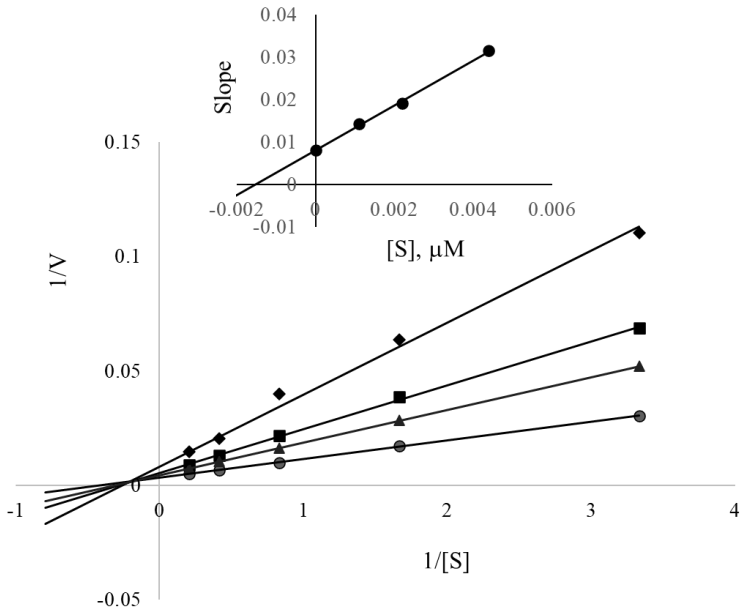

Computational analyses

Quantitative structure-activity relationship (QSAR) analyses and 3D-QSAR analyses were applied to further understand the inhibition of MAO-B by the 3-styrylchromone derivatives.

QSAR analyses

QSAR analyses of 3-styrylchromone derivatives were conducted using Molecular Operating Environment (MOE) [14] and Dragon [15] (a total of 3,132 descriptors) with pIC_{50} value for MAO-B inhibitory activity. A total of 1,796 descriptors showed significant correlations ($P < 0.05$) for MAO-B inhibitory activity. The scatter plots of the top six descriptors are shown in Fig. 3. The strongly correlated descriptors indicated that properties, such as 3-dimensional (3D) shape, size, polarizability, and hydrophobic and lipophilic properties, of 3-styrylchromone derivatives are important for their inhibitory activity against MAO-B. RDF, TDB and vsurf descriptors were useful for the evaluation of 3D structures. These structural and physicochemical properties suggested that the binding of 3-styrylchromone derivatives to the binding site of MAO-B is stabilized by van der Waals forces, electrostatic interactions, and 3D structures.

Fig. 3

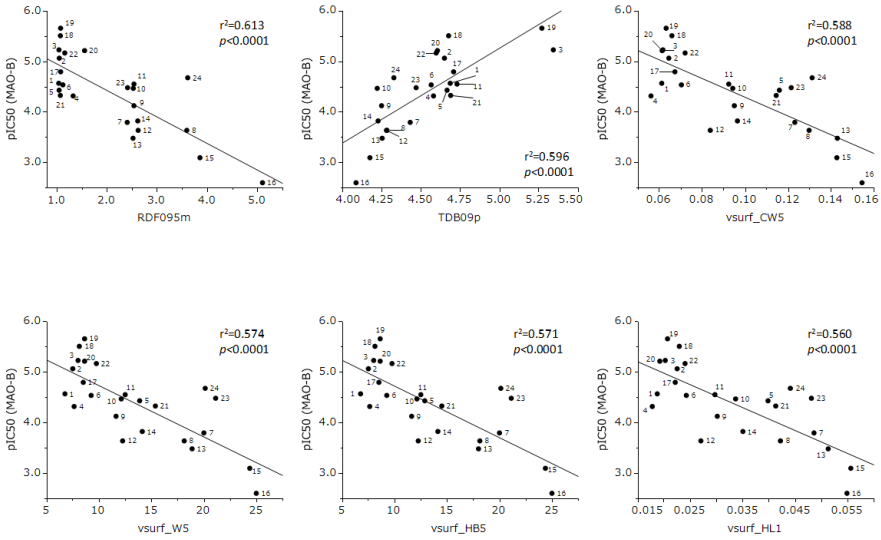

RDF095m	3D shape and size	RDF descriptors	Radial Distribution Function - 095 / weighted by mass
TDB09p	3D shape and polarizability	3D autocorrelations	3D Topological distance based descriptors - lag 9 weighted by polarizability
vsurf_CW5	Capacity factor	Surface Area, Volume and Shape Descriptors	The vsurf_ descriptors are similar to the VolSurf descriptors ; these descriptors have been shown to be useful in pharmacokinetic property prediction.
vsurf_W5	Hydrophilic volume	Surface Area, Volume and Shape Descriptors	
vsurf_HB5	H-bond donor capacity	Surface Area, Volume and Shape Descriptors	
vsurf_HL1	Hydrophilic-Lipophilic	Surface Area, Volume and Shape Descriptors	

3D-QSAR analyses

Further 3D-QSAR analyses of the MAO-B inhibitory activities of 3-styrylchromone derivatives were conducted with AutoGPA using MOE [16]. The developed models predicted pIC_{50} values for MAO-B that corresponded with the experimental values, as shown in Fig. 4. The pIC_{50} values of MAO-B had a determination coefficient (R^2) of 0.972 and Leave-One-Out cross-validated determination coefficients (Q^2) of 0.914. In this analysis, $Q^2 > 0.5$ suggested that the model was reasonable and would have good predictive ability [17]. The model for MAO-B inhibitory activity provided reasonable pIC_{50} values.

Fig. 4

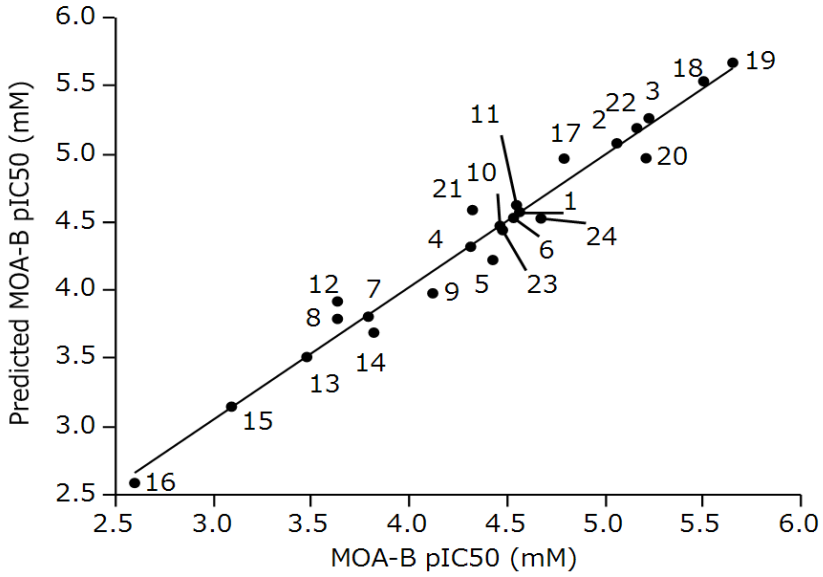

The contour map of the AutoGPA-based models of MAO-B pIC_{50} value is shown in Fig. 5A. In this figure, the blue contour suggests an electropositive charge and the red contour suggests an electronegative charge that increases MAO-B inhibitory activity; in the steric contour map, the green contour represents bulky groups that increase activity, and the yellow contour indicates groups that decrease activity. Molecular docking studies performed using the MOE-Dock function were conducted to better understand the developed models (Fig. 5B, C).

Fig. 5A

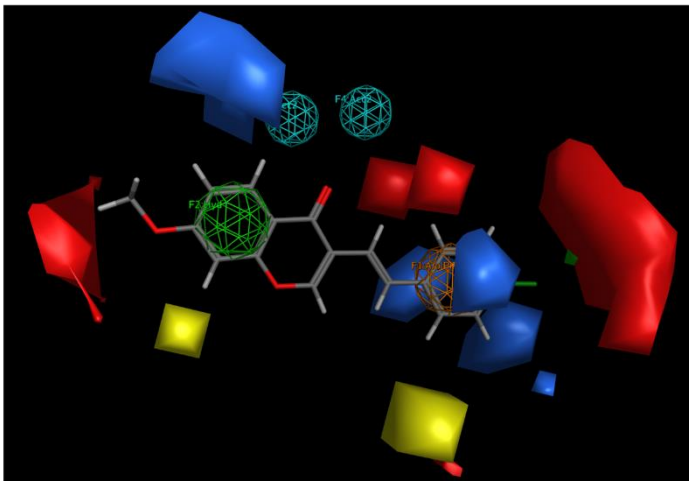

Fig. 5B

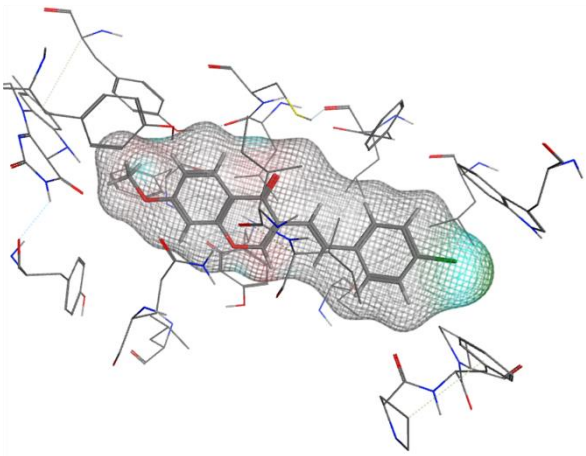

Fig. 5C

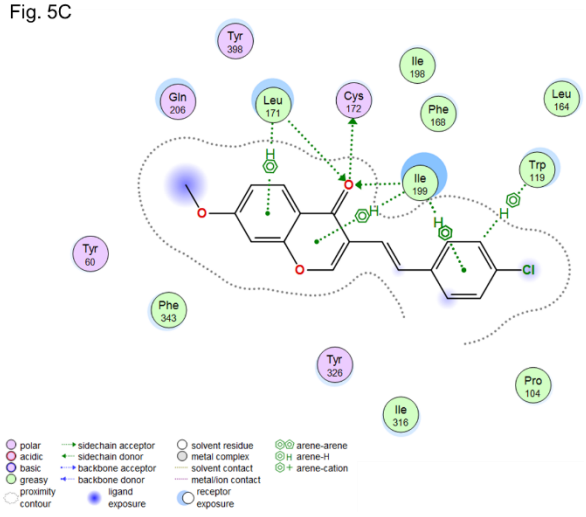

Interactions between compound **19** and MAO-B protein (PDB code 4A79) were investigated using MOE. In the model, the interaction of compound **19** with pharmacophore F1 corresponds to Ile199, and F2 corresponds to Leu171 as F3. The pharmacophore F4 corresponds to Cys172. The large red contour close to chlorine on phenyl ring suggested that halogenation at R^4 on the phenyl ring might increase the MAO-B inhibitory activity. The red contour close to the chromone ring corresponds to FAD. This supported the result that the methoxy substitution on the chromone ring at R^2 increase MAO-B inhibitory activity of compound **19**. We reported 2-styrylchromone derivatives as MAO-B selective inhibitors [9], with 6-methoxy-4'-chloro-2-styrylchromone being a potent inhibitor. Comparison of compound **19** showed that diagonal substitution on the chromone ring increased MAO-B inhibitory activity.

In a recent review by Manzoor and Hoda [3], it was reported that both MAO-A and MAO-B active site residues have well-related hydrophobic amino acids in the substrate-binding domain, mainly converted from aliphatic and aromatic residues, such as Tyr60, Phe168, Tyr188, Ile198, Gln206, Phe343, Tyr398 and Tyr435. These residues are shown in Fig.5C and indicate that compound **19** is tightly bound to the MAO-B active site. The MAO-A active site also had these amino acids residues; thus, several 3-styrylchromone derivatives might show strong inhibitory activity against MAO-A. The other amino acid residues in the MAO-B active site were Leu171, Cys172, Ile199 and Tyr326; these are shown in Fig.5C. Ile199 and Ty326 are important residues in MAO-B active site for the regulation of the active site cavity volume. The interaction of compound **19** with these residues might induce a conformational change in the MAO-B active site to increase the inhibitory activity. The other important residues in the MAO-B active site were Tyr398 and Tyr435, which made substrate binding cages for the location and recognition of substrate's amino group. In a recent docking study by Reis *et al*., of *N*-(3'-chlorophenyl)-4-oxo-4H-chromene-3-carboxamide and *N*-(3'-fluorophenyl)-4-oxo-4H-chromene-3-carboxamide with MAO-B, a shift in the position of Pro104-Pro105 toward inhibitor was observed [13]. This suggests that Pro104-Pro105 interacted with the halogen on the phenyl ring, increasing the binding. Compound **19** might also interact with Pro104.

These results suggest that the structure of 3-styrylchromone may be a useful scaffold for the design and development of novel MAO-B inhibitors.

In conclusion

The present study showed that 3-styrylchromone derivatives to be potent and selective

MAO-B inhibitors. Of the 24 synthesized derivatives, most showed significant MAO-B inhibitory activities, except compound **21**, which showed strong MAO-A inhibitory activity. Compound **19**, having a methoxy group at R^2 and chlorine at R^4, showed the highest MAO-B inhibitory activity. Computational analyses also suggested the influence of substitution by the methoxy group at R^2 and chlorine at R^4. QSAR and 3D-QSAR analyses suggested that 3-styrylchromone derivatives are promising scaffolds for the design and development of new MAO-B inhibitors.

Experimental

Chemistry

All reagents and solvents were purchased from commercial sources. Analytical thin-layer chromatography was performed on silica-coated plates (silica gel 60 F-254; Merck Ltd., Tokyo, Japan) and visualized under UV light. Column chromatography was carried out using silica gel (Wakogel C-200; Wako Pure Chemical Industry Co., Osaka, Japan). All melting points were determined using a Yanagimoto micro-hot stage and were uncorrected. ^{1}H NMR and ^{13}C NMR spectra were recorded on a Varian 400-MR spectrometer using tetramethylsilane as an internal standard. MS spectra were measured using a JEOL JMS-700 spectrometer. Elemental analyses were carried out on a Yanaco CHN MT-6 elemental analyzer.

Synthesis of 3-formylchromones (**IIa-c**)

3-Formylchromones **IIa** and **IIb** were synthesized according to a previously reported method [11]. 3-Formylchromone **IIc** was synthesized via difluorodioxaborin of 2-hydroxy-4-methoxyacetophenone (**Ic**) according to the method described by Yan *et al*. [12]. The products (**IIa-c**) were identified by their melting points and ^{1}H-NMR spectra.

Synthesis of 4-(methoxymethoxy)benzeneacetic acid (**IIIj**)

A mixture of 4-hydroxyphenylacetic acid (**IIIe**, 10 mmol) and conc. H_2SO_4 (0.5 mmol) in MeOH (50 mL) was refluxed for 1 h. After evaporation of the solvent under reduced pressure, the residue was diluted with water and extracted with AcOEt. The organic layer was dried over Na_2SO_4 and the solvent was evaporated under reduced pressure. The residue was dissolved in acetone (50 mL) and then chloromethyl methyl ether (20 mmol) and K_2CO_3 (30 mmol) was added. The mixture was heated at gentle reflux for 16 h. After filtration of K_2CO_3, the solvent was evaporated under reduced pressure. The residue was passed once through a short silica gel column (Hexane : AcOEt = 15 : 1) and the solvent was evaporated. The obtained compound (10 mmol) was dissolved in MeOH-H_2O (9 : 1, 68 mL) and KOH (100 mmol) was added. The mixture was stirred for 30 min at room temperature. After evaporation of the solvent under reduced pressure, the residue was diluted with water and acidified with 4 M HCl. The whole was extracted with AcOEt. The organic layer was dried over Na_2SO_4 and the solvent was evaporated under reduced pressure. The residue was purified by silica gel column chromatography (hexane-AcOEt solvent system) to give the title compound (**IIIj**) in 78% yield. Colorless powder. mp 42-43 ºC. ^{1}H NMR ($CDCl_3$, 400 MHz) δ 7.21 (2H, d, J = 8.8 Hz, H-2, H-5), 7.01 (2H, d, J = 8.8 Hz, H-2, H-5), 5.17 (2H, s, -OCH_2O-), 3.60 (2H, s, CH_2),

3.47 (3H, s, OCH_3). ^{13}C NMR ($CDCl_3$, 100 MHz) δ 177.4, 156.7, 130.6, 126.7, 116.6, 94.6, 56.1, 40.2. MS (EI) *m/z* 196 $[M]^+$. *Anal.* Calcd for $C_{10}H_{12}NO_4$: C, 61.22; H, 6.16. Found: C, 61.30; H, 6.14.

Synthesis of (*E*)-3-styryl-4*H*-1-benzopyran-4-ones (**1**-**24**)

Compounds **2**, **3**, **5**-**8**, **10**, **11**, and **13**-**16** were synthesized as described in a previous report [11]. Compounds **1**, **9**, and **17** were synthesized using a previously reported method with a small modification, involuving the use of phenylmalonic acids. Briefly, the corresponding 3-formylchromone (**II**, 2 mmol) and phenylmalonic acid (**IIIa**, 8 mmol) were dissolved in dry pyridine (20 mL). *tert*-BuOK (3 mmol) was added to the solution, and the mixture was refluxed until complete disappearance of 3-formylchromone. After the reaction mixture was diluted with ice-water and acidified to pH 4 with 5 M HCl, the sample was extracted with $CHCl_3$. The combined organic layer was washed with a saturated $NaHCO_3$ solution followed by brine. The organic layer was dried over Na_2SO_4, and the solvent was evaporated under reduced pressure. The residue was purified by silica gel column chromatography (hexane-AcOEt solvent system) to obtain the corresponding 3-styryl-4*H*-1-benzopyran-4-one derivative.

Compound **4**, **12**, and **18**-**24** were synthesized using a previously reported method [11].

The newly synthesized products were identified by elemental analyses, ^1H- and ^{13}C-NMR spectra.

Synthesis of 3-styrylchromone having a hydroxy group (**21**)

According to a previously reported method [11], 3-formylchromne (**IIc**, 2 mmol) and protected 4-hydroxyphenylacetic acid (**IIIj**, 4 mmol) were treated with *tert*-BuOK (3 mmol), and then the obtained compound (**21'**, 1 mmol) was dissolved in MeOH (18 mL) and 10% HCl (8 mL) was added. The mixture was heated at gentle reflux for 15 min. After evaporation of the solvent under reduced pressure, the residue was diluted with water and extracted with AcOEt. The organic layer was dried over Na_2SO_4 and the solvent was evaporated under reduced pressure. The residue was purified by silica gel column chromatography (hexane-AcOEt solvent system) to give the title compound (**21**).

3-[(1*E*)-2-Phenylethenyl]-4*H*-1-benzopyran-4-one (**1**)

Yield 92%. white scales. mp 167-169 ºC (lit. 169-170 [18]). ^1H NMR ($CDCl_3$, 400 MHz) δ 8.32 (1H, dd, *J* = 8.0, 1.7 Hz, H-5), 8.13 (1H, d, *J* = 0.7 Hz, H-2), 7.68 (ddd, *J* = 8.5, 7.1, 1.7 Hz, H-7), 7.64 (d, *J* = 16.4 Hz, H-β), 7.54 (2H, m, H-2', H-6'), 7.48 (1H,

dd, *J* = 8.5, 1.0 Hz, H-8), 7.44 (1H, ddd, *J* = 8.0, 7.1, 1.0 Hz, H-6), 7.36 (2H, m, H-3', H-5'), 7.27 (1H, m, H-4'), 7.00 (1H, dd, *J* = 16.4, 0.7 Hz, H-α). MS (EI) *m/z* 248 $[M]^+$. The ^{1}H-NMR spectrum was similar to that previously reported [18].

3-[(1*E*)-2-(4-Dimethylaminophenyl)ethenyl]-4*H*-1-benzopyran-4-one (**4**)
Yield 48%. yellow needles. mp 191-193 ºC. ^{1}H NMR ($CDCl_3$, 400 MHz) δ 8.30 (1H, dd, *J* = 8.0, 1.7 Hz, H-5), 8.09 (1H, d, *J* = 0.7 Hz, H-2), 7.65 (1H, ddd, *J* = 8.5, 7.1, 1.7 Hz, H-7), 7.47 (1H, d, *J* = 16.3 Hz, H-β), 7.47-7.39 (4H, m, H-6, H-8, H-2', H-6'), 6.83 (1H, dd, *J* = 16.3, 0.7 Hz, H-α), 6.71 (2H, d, *J* = 8.6 Hz, H-3', H-5'), 2.99 (6H, s, NMe_2). ^{13}C NMR ($CDCl_3$, 100 MHz) δ 176.7, 155.8, 151.8, 150.3, 133.2, 131.5, 127.7, 126.2, 125.7, 125.0, 124.0, 122.6, 118.0, 114.3, 112.3, 40.4. MS (EI) *m/z* 291 $[M]^+$. *Anal.* Calcd for $C_{19}H_{17}NO_2$: C, 78.33; H, 5.88; N, 4.81. Found: C, 78.47; H, 5.83; N, 4.67.

6-Methoxy-3-[(1*E*)-2-phenylethenyl]-4*H*-1-benzopyran-4-one (**9**)
Yield 65%. pale orange needles. mp 132-134 ºC (lit. 123-126 [19]). ^{1}H NMR ($CDCl_3$, 400 MHz) δ 8.12 (1H, d, *J* = 0.7 Hz, H-2), 7.67 (1H, d, *J* = 3.1 Hz, H-5), 7.63 (1H, d, *J* = 16.3 Hz, H-β), 7.53 (2H, m, H-2', H-6'), 7.42 (1H, d, *J* = 9.1 Hz, H-8), 7.37 (2H, m, H-3', H-5'), 7.28 (1H, m, H-4'), 7.27 (1H, dd, *J* = 9.1, 3.1 Hz, H-7), 7.01 (1H, dd, *J* = 16.3, 0.7 Hz, H-α), 3.92 (3H, s, OMe). MS (EI) *m/z* 278 $[M]^+$. The ^{1}H-NMR spectrum was similar to that previously reported [19].

3-[(1*E*)-2-(4-Dimethylaminophenyl)ethenyl]-6-methoxy-4*H*-1-benzopyran-4-one (**12**)
Yield 63%. orange needles. mp 175-177 ºC. ^{1}H NMR ($CDCl_3$, 400 MHz) δ 8.08 (1H, s, H-2), 7.65 (1H, d, *J* = 3.1 Hz, H-5), 7.46 (1H, d, *J* = 16.5 Hz, H-β), 7.43 (2H, d, *J* = 8.8 Hz, H-2', H-6'), 7.39 (1H, d, *J* = 9.1 Hz, H-8), 7.25 (1H, dd, *J* = 9.1, 3.1 Hz, H-7), 6.84 (1H, d, *J* = 16.5 Hz, H-α), 6.71 (2H, d, *J* = 8.8 Hz, H-3', H-5'), 3.92 (3H, s, OMe), 2.99 (6H, s, NMe_2). ^{13}C NMR ($CDCl_3$, 100 MHz) δ 176.5, 156.8, 151.7, 150.7, 150.2, 131.4, 127.7, 125.8, 124.6, 123.5, 121.8, 119.4, 114.4, 112.3, 105.1, 55.9, 40.4. MS (EI) *m/z* 321 $[M]^+$. *Anal.* Calcd for $C_{20}H_{19}NO_3$: C, 74.75; H, 5.96; N, 4.36. Found: C, 74.83; H, 5.94; N, 4.19.

7-Methoxy-3-[(1*E*)-2-phenylethenyl]-4*H*-1-benzopyran-4-one (**17**)
Yield 81%. yellow needles. mp 144-146 ºC (151-152 [19]). ^{1}H NMR ($CDCl_3$, 400 MHz) δ 8.21 (1H, d, *J* = 8.9 Hz, H-5), 8.05 (1H, d, *J* = 0.7 Hz, H-2), 7.61 (1H, d, *J* = 16.3 Hz, H-β), 7.53 (2H, m, H-2', H-6'), 7.36 (2H, m, H-3', H-5'), 7.27 (1H, m, H-4'), 7.00 (1H, dd, *J* = 8.9, 2.4 Hz, H-6), 6.97 (1H, dd, *J* = 16.3, 0.7 Hz, H-α), 6.85 (1H, d, *J*

= 2.4 Hz, H-8), 3.91 (3H, s, OMe). MS (EI) *m/z* 278 $[M]^+$. The ^{1}H-NMR spectrum was similar to that previously reported [19].

3-[(1*E*)-2-(4-Fluorophenyl)ethenyl]-7-methoxy-4*H*-1-benzopyran-4-one (**18**)
Yield 75%. pale yellow needles. mp 165-168 ºC. ^{1}H NMR ($CDCl_3$, 400 MHz) δ 8.20 (1H, d, *J* = 8.9 Hz, H-5), 8.03 (1H, d, *J* = 0.7 Hz, H-2), 7.60 (1H, d, *J* = 16.3 Hz, H-β), 7.47 (2H, m, H-2', H-6'), 7.05 (2H, m, H-3', H-5'), 7.00 (1H, dd, *J* = 8.9, 2.4 Hz, H-6), 6.87 (1H, dd, *J* = 16.3, 0.7 Hz, H-α), 6.85 (1H, d, *J* = 2.4 Hz, H-8), 3.91 (3H, s, OMe). ^{13}C NMR ($CDCl_3$, 100 MHz) δ 176.0, 164.0, 162.4 (d, $^1J_{C\text{-}F}$ = 250 Hz), 157.5, 152.5, 133.6, 130.3, 128.1 (d, $^3J_{C\text{-}F}$ = 8 Hz), 127.6, 121.5, 118.9, 118.0, 115.6 (d, $^2J_{C\text{-}F}$ = 22 Hz), 114.7, 100.1, 55.8. MS (EI) *m/z* 296 $[M]^+$. *Anal.* Calcd for $C_{18}H_{13}FO_3$: C, 72.97; H, 4.42. Found: C, 73.21; H, 4.48.

3-[(1*E*)-2-(4-Chlorophenyl)ethenyl]-7-methoxy-4*H*-1-benzopyran-4-one (**19**)
Yield 64%. pale yellow needles. mp 171-173 ºC (lit. 165-166 [20]). ^{1}H NMR ($CDCl_3$, 400 MHz) δ 8.20 (1H, d, *J* = 8.9 Hz, H-5), 8.03 (1H, d, *J* = 0.7 Hz, H-2), 7.61 (1H, d, *J* = 16.3 Hz, H-β), 7.44 (2H, d, *J* = 8.5 Hz, H-2', H-6'), 7.32 (2H, d, *J* = 8.5 Hz, H-3', H-5'), 7.00 (1H, dd, *J* = 8.9, 2.4 Hz, H-6), 6.92 (1H, dd, *J* = 16.3, 0.7 Hz, H-α), 6.85 (1H, d, *J* = 2.4 Hz, H-8), 3.91 (3H, s, OMe). MS (EI) *m/z* 312 $[M]^+$. The ^{1}H-NMR spectrum was similar to that previously reported [20].

3-[(1*E*)-2-(4-Dimethylaminophenyl)ethenyl]-7-methoxy-4*H*-1-benzopyran-4-one (**20**)
Yield 62%. yellow needles; mp 202 ºC; ^{1}H NMR ($CDCl_3$, 400 MHz) δ 8.20 (1H, d, *J* = 8.9 Hz, H-5), 8.02 (1H, d, *J* = 0.7 Hz, H-2), 7.45 (1H, d, *J* = 16.3 Hz, H-β), 7.42 (2H, d, *J* = 8.8 Hz, H-2', H-6'), 6.98 (1H, dd, *J* = 8.9, 2.4 Hz, H-6), 6.84 (1H, d, *J* = 2.4 Hz, H-8), 6.82 (1H, dd, *J* = 16.3, 0.7 Hz, H-α), 6.72 (2H, d, *J* = 8.8 Hz, H-3', H-5'), 3.91 (3H, s, OMe), 2.98 (6H, s, NMe_2). ^{13}C NMR ($CDCl_3$, 100 MHz) δ 176.2, 163.8, 157.6, 151.3, 150.2, 131.3, 127.7, 127.6, 125.8, 122.5, 118.0, 114.5, 114.4, 112.3, 100.0, 55.8, 40.4. MS (EI) *m/z* 321 $[M]^+$. *Anal.* Calcd for $C_{20}H_{19}NO_3$: C, 74.75; H, 5.96; N, 4.36. Found: C, 74.53; H, 5.87; N, 4.15.

3-[(1*E*)-2-(4-Hydroxyphenyl)ethenyl]-7-methoxy-4*H*-1-benzopyran-4-one (**21**)
Yield 21% (2 steps). yellow powder. mp 126 ºC. ^{1}H NMR (DMSO-d_6, 400 MHz) δ 9.72 (1H, br. s, OH), 8.54 (1H, s, H-2), 8.04 (1H, d, *J* = 8.9, H-5), 7.57 (1H, d, *J* = 16.3 Hz, H-β), 7.37 (2H, d, *J* = 8.8 Hz, H-2', H-6'), 7.15 (1H, d, *J* = 2.4 Hz, H-8), 7.09 (1H, dd, *J* = 8.9, 2.4 Hz, H-6), 6.82 (1H, d, *J* = 16.3 Hz, H-α), 6.79 (2H, d, *J* = 8.8 Hz, H-3', H-5'),

3.90 (3H, s, OMe). MS (EI) *m/z* 299 $[M]^+$.
^{13}C NMR (DMSO-d_6, 100 MHz) δ 175.0, 163.7, 157.4, 157.1, 153.9, 130.6, 128.3, 127.7, 126.8, 120.8, 117.2, 116.1, 115.6, 114.9, 100.6, 56.1. MS (EI) *m/z* 294 $[M]^+$. *Anal.* Calcd for $C_{18}H_{14}O_4$: C, 73.46; H, 4.79. Found: C, 73.58; H, 4.89.

7-Methoxy-3-[(1*E*)-2-(4-methoxyphenyl)ethenyl]-4*H*-1-benzopyran-4-one (**22**)
Yield 55%. yellow needles. mp 173 ºC. ^1H NMR ($CDCl_3$, 400 MHz) δ 8.20 (1H, d, *J* = 8.9 Hz, H-5), 8.02 (1H, d, *J* = 0.7 Hz, H-2), 7.52 (1H, d, *J* = 16.3 Hz, H-β), 7.46 (2H, d, *J* = 8.7 Hz, H-2', H-6'), 6.99 (1H, dd, *J* = 8.9, 2.4 Hz, H-6), 6.89 (2H, d, *J* = 8.7 Hz, H-3', H-5'), 6.85 (1H, dd, *J* = 16.3, 0.7 Hz, H-α), 6.84 (1H, d, *J* = 2.4 Hz, H-8), 3.91 (3H, s, OMe), 3.83 (3H, s, OMe). ^{13}C NMR ($CDCl_3$, 100 MHz) δ 176.1, 163.9, 159.4, 157.5, 152.0, 130.9, 130.2, 127.8, 127.6, 122.0, 118.0, 116.9, 114.6, 114.1, 100.1, 55.8, 55.3. MS (EI) *m/z* 308 $[M]^+$. *Anal.* Calcd for $C_{19}H_{16}O_4$: C, 74.01; H, 5.23. Found: C, 73.71; H, 5.22.

3-[(1*E*)-2-(3,4-Dimethoxyphenyl)ethenyl]-7-methoxy-4*H*-1-benzopyran-4-one (**23**)
Yield 24%. pale yellow powder. mp 142-143 ºC. ^1H NMR ($CDCl_3$, 400 MHz) δ 8.20 (1H, d, *J* = 8.9 Hz, H-5), 8.04 (1H, d, *J* = 0.7 Hz, H-2), 7.51 (1H, d, *J* = 16.3 Hz, H-β), 7.09 (1H, d, *J* = 2.0 Hz, H-2'), 7.05 (1H, dd, *J* = 8.2, 2.0 Hz, H-6'), 7.00 (1H, dd, *J* = 8.9, 2.4 Hz, H-6), 6.87 (1H, dd, *J* = 16.3, 0.7 Hz, H-α), 6.88-6.84 (2H, m, H-8, H-5'), 3.94 (3H, s, OMe), 3.91 (3H, s, OMe), 3.90 (3H, s, OMe). ^{13}C NMR ($CDCl_3$, 100 MHz) δ 176.1, 163.9, 157.6, 152.0, 149.07, 149.03, 131.1, 130.5, 127.6, 121.9, 120.0, 118.0, 117.0, 114.6, 111.1, 108.8, 100.1, 55.91, 55.87, 55.81. MS (EI) *m/z* 338 $[M]^+$. *Anal.* Calcd for $C_{20}H_{18}O_5$: C, 71.00; H, 5.36. Found: C, 71.17; H, 5.37.

7-Methoxy-3-[(1*E*)-2-(3,4,5-trimethoxyphenyl)ethenyl]-4*H*-1-benzopyran-4-one (**24**)
Yield 58%. pale orange needles. mp 161-163 ºC. ^1H NMR ($CDCl_3$, 400 MHz) δ 8.21 (1H, d, *J* = 8.9 Hz, H-5), 8.05 (1H, d, *J* = 0.7 Hz, H-2), 7.56 (1H, d, *J* = 16.3 Hz, H-β), 7.01 (1H, dd, *J* = 8.9, 2.4 Hz, H-6), 6.89 (1H, dd, *J* = 16.3, 0.7 Hz, H-α), 6.86 (1H, d, *J* = 2.4 Hz, H-8), 6.75 (2H, s, H-2', H-6'), 3.92 (3H, s, OMe), 3.91 (6H, s, OMe, OMe), 3.87 (3H, s, OMe). ^{13}C NMR ($CDCl_3$, 100 MHz) δ 176.0, 164.0, 157.6, 153.3, 152.4, 138.0, 133.1, 131.4, 127.6, 121.6, 118.5, 118.0, 114.7, 103.6, 100.1, 61.0, 56.1 (2C), 55.8. MS (EI) *m/z* 368 $[M]^+$. *Anal.* Calcd for $C_{21}H_{20}O_6$: C, 68.47; H, 5.47. Found: C, 68.72; H, 5.52.

Biological Assays

Recombinant human monoamine oxidase A (MAO-A), recombinant human MAO-B, pargyline, and kynuramine were purchased from Sigma-Aldrich Japan Co., Tokyo, Japan.

MAO Inhibitory Assay

MAO inhibitory activity was assayed using a previously reported method [9,10]. Briefly, 140 μL of 0.1 M potassium phosphate buffer (pH 7.4), 8 μL of 0.75 mM kynuramine, and 2 μL of a dimethyl sulfoxide (DMSO) inhibitor solution, were preincubated at 37°C for 10 min. Diluted human recombinant enzyme (50 μL) was then added to obtain a final protein concentration of 0.0075 mg/mL (MAO-A) or 0.015 mg/mL (MAO-B) in the assay mixture. The reaction mixture was further incubated at 37°C and the reaction was stopped after 20 min by the addition of 75 μL of 2 M NaOH. The fluorescent product generated by MAO, 4-quinolinol, was measured at excitation and emission wavelengths of 310 nm and 400 nm, respectively, using a microplate reader (Molecular Devices SPECTRA MAX M2). Each data point was measured from triplicate samples. The sample solution was replaced with DMSO to provide a negative control, and pargyline, safinamide, and chlorgyline were used as positive controls. The IC_{50} values were calculated from a line through two points that sandwiched the point corresponding to 50% inhibition (IC_{50}) by plotting the remained activity (%) related to the control (100%) versus the logarithm of the inhibitor concentration to obtain a sigmoidal dose-response curve.

Lineweaver–Burk plots

The inhibition of MAO-B by compounds **1** and **19** was determined by constructing a set of four Lineweaver–Burk plots. The first plot was constructed in the absence of inhibitor, and the remaining three plots were constructed in the presence of various concentrations of the test inhibitor: 1/2 x IC_{50}, 1 x IC_{50} and 2 x IC_{50} (IC_{50} = 0.027 μM for compound **1** and 0.0022 μM for compound **19**). The enzyme substrate kynuramine was used at concentrations ranging from 3.75 to 120 μM.

Calculation of chemical descriptors

Each 3D chemical structure (Marvin Sketch ver 16; ChemAxon, Budapest, Hungary, http://www.chemaxon.com) was optimized by CORINA Classic (Molecular Networks GmbH, Nürnberg, Germany) with forcefield calculations (amber-10: EHT) in Molecular Operating Environment (MOE) version 2019.0102 (Chemical Computing Group Inc., Quebec, Canada) [14]. The number of structural descriptors calculated from MOE and

Dragon 7.0 (Kode srl., Pisa, Italy) [15] was 354 and 5,255, respectively, of which 269 and 2,863 (total 3,132) descriptors were used for analysis.

3D-QSAR and docking analyses

AutoGPA in MOE can automatically generate 3D-QSAR models based on the chemical structures and biological activities for sets of inhibitors [16, 17]. The CoMFA algorithm was employed to develop 3D-QSAR models. Docking analysis was carried out with MAO-B protein (PDB code 4A79) using MOE.

Statistical analysis

The relation between the substituents and the MAO-related properties, such as IC_{50} values and MAO-B selectivity, was analyzed with the Wilcoxon signed-rank test. The relationship between the chemical descriptors and MAO-B-related properties was investigated using Pearson's correlation analysis. These statistical calculations were performed by JMP Pro version 15.0.0 (SAS Institute Inc., Cary, NC, USA), with significance considered at $p<0.05$.

References

[1] K. F. Tipton, 90 years of monoamine oxidase: some progress and some confusion, J. Neural. Transm. (Vienna), 125 (11) (2018) 1519-1551.

[2] L.G. Iacovino, F. Magnani, C. Binda, The structure of monoamine oxidases: past, present, and future, J. Neural. Transm. (Vienna), 125 (11) (2018) 1567-1579.

[3] S. Manzoor, N. Hoda, A comprehensive review of monoamine oxidase inhibitors as Anti-Alzheimer's disease agents: A review, Eur. J. Med. Chem., 206 (2020) 112787.

[4] A. Gaspar, T. Silva, M. Yáñez, D. Vina, F. Orallo, F. Ortuso, E. Uriarte, S. Alcaro, F. Borges, Chromone, a privileged scaffold for the development of monoamine oxidase inhibitors, J. Med. Chem., 54 (14) (2011) 5165-73.

[5] A. Gaspar, M.J. Matos, J. Garrido, E. Uriarte, F. Borges, Chromone: a valid scaffold in medicinal chemistry, Chem. Rev., 114 (9) (2014) 4960-92.

[6] J. Reis, A. Gaspar, N. Milhazes, F. Borges, Chromone as a Privileged Scaffold in Drug Discovery: Recent Advances, J. Med. Chem., 60 (19) (2017) 7941-7957.

[7] K. Takao, T. Saito, D. Chikuda, Y. Sugita, 2-Azolylchromone Derivatives as Potent and Selective Inhibitors of Monoamine Oxidases A and B, Chem. Pharm. Bull. (Tokyo), 64 (10) (2016) 1499-1504.

[8] K. Takao, H. Yahagi, Y. Uesawa, Y. Sugita, 3-(*E*)-Styryl-2*H*-chromene derivatives as potent and selective monoamine oxidase B inhibitors., Bioorg. Chem., 77 (2018) 436-442. doi: 10.1016/j.bioorg.2018.01.036.

[9] K. Takao, S. Endo, J. Nagai, H. Kamauchi, Y. Takemura, Y. Uesawa, Y. Sugita, 2-Styrylchromone derivatives as potent and selective monoamine oxidase B inhibitors, Bioorg. Chem., 92 (19) 103285.

[10] K. Takao, T. Sakatsume, H. Kamauchi, Y. Sugita, Syntheses and evaluation of 2- or 3-(*N*-cycloamino)chromone derivatives as monoamine oxidase inhibitors, Chem. Pharm. Bull. (Tokyo), 68 (11) (2020) 1082-1089.

[11] K. Takao, R. Ishikawa, Y. Sugita, Synthesis and biological evaluation of 3-styrylchromone derivatives as free radical scavengers and α-glucosidase inhibitors, Chem. Pharm. Bull. (Tokyo), 62 (8) (2014) 810-815.

[12] J. Yan, L. Fan, J. Qin, C. Li, Z. Yang, A novel and resumable Schiff-base fluorescent chemosensor for Zn(II), Tetrahedron Lett., 57 (2016) 2910–2914.

[13] J. Reis, N. Manzella, F. Cagide, J. Mialet-Perez, E. Uriarte, A. Parini, F. Borges, C. Binda, Tight-Binding Inhibition of Human Monoamine Oxidase B by Chromone Analogs: A Kinetic, Crystallographic, and Biological Analysis, J. Med. Chem. 61 (2018) 4203-4212.

[14] Calculate Descriptors, MOE2015.10 on-line help manual, Chemical Computing

Group.
[15] https://chm.kode-solutions.net/products_dragon_descriptors.php
[16] N. Asakawa, S. Kobayashi, J. Goto, N. Hirayama, AutoGPA: An Automated 3D-QSAR Method Based on Pharmacophore Alignment and Grid Potential Analysis., Int. J. Med. Chem. 2012 (2012) 498931. doi: 10.1155/2012/498931.
[17] F. Y. Guo, Q. Y. Yan, K. Lin, W. Y. Hong, G.S. Yang, AutoGPA-Based 3D-QSAR Modeling and Molecular Docking Study on Factor Xa Inhibitors as Anticoagulant Agents., MATEC Web of Conferences, 44 (2016) 02018.
[18] Dawood K. M., Microwave-assisted Suzuki-Miyaura and Heck-Mizoroki cross-coupling reactions of aryl chlorides and bromides in water using stable benzothiazole-based palladium(II) precatalysts., Tetrahedron, 63 (2007) 9642–9651.
[19] T. Patonay, A. Kiss-Szikszai, V. M. L. Silva, A. M. S. Silva, D. C. G. A. Pinto, J. A. S. Cavaleiro, J. Jeko, Microwave-Induced Synthesis and Regio- and Stereoselective Epoxidation of 3-Styrylchromones., Eur. J. Org. Chem., (2008) 1937–1946.
[20] V. L. M. Silva, A. M. S. Silva, D. C. G. A. Pinto, J. A. S. Cavaleiro, A. Vasas, T. Patonay, Syntheses of (E)- and (Z)-3-styrylchromones., Monatsh. Chem., 139, (2008) 1307–1315.

Table Captions and Figure Legends

Chart 1 Synthesis protocol for 3-styrylchromone derivatives.
Reagents and conditions: (a) DMF/$POCl_3$; (b) $(CH_3CO)_2O/BF_3Et_2O$; (c) *tert*-BuOK, dry pyridine, reflux; (d) allylbromide, K_2CO_3, EtOH and then KOH; (e) conc. H_2SO_4, MeOH, reflux; (f) chloromehyl methyl ether, K_2CO_3, acetone, reflux and then KOH, MeOH-H_2O; (g) $Pd(PPh_3)_4$, morpholine, THF, 60°C; (h) 10% HCl, MeOH, reflux.

Table 1 The IC_{50} values and selectivities of 3-styrylchromone derivatives for the inhibition of MAO-A and MAO-B.
MAO-B selectivity is given as the ratio of the IC_{50} value for MAO-A and IC_{50} value for MAO-B. All values are expressed as the mean ± standard deviation of triplicate determinations.

Fig. 1 Effect of substitutions at R^1, R^2, R^3, R^4 and R^5 of 3-styrylchromone derivatives on MAO-A (A) and MAO-B (B) inhibitory activity.

Fig. 2 Lineweaver–Burk plots for the inhibition of MAO-B by compound **1** and **19**. The plots were constructed in the absence (filled circles) and presence (other symbols) of various concentrations of compound **1** (A) or **19** (B). The inset is a graph of the slopes of the Lineweaver–Burk plots versus inhibitor concentration (Ki = 0.019 μM for compound **1** and 0.0015 μM for compound **19**). The rate (V) is expressed as % of control. Kynuramine was used at 30 μM.

Fig. 3 Determination of the correlation between the chemical descriptors and the pIC_{50} values of 3-styrylchromone derivatives for MAO-B.

Fig. 4 Graph of the predicted and experimental pIC_{50} MAO-B inhibition values for 3-styrylchromone derivatives.

Fig. 5 AutoGPA model and docking results obtained from a set of 3-styrylchromone derivatives as MAO-B inhibitors. (A) AutoGPA steric and electrostatic contours field plot. The position and structure of 3-styrylchromone are superposed. Green and yellow contours indicate regions where bulky groups increase and decrease activity, respectively. Blue and red contours indicate regions where positive and negative electrostatic groups increase activity. (B) Ligand interaction graph of the active pocket

of MAO-B with compound **19**. (C) 2D interaction diagram of compound **19** with the MAO-B binding cavity.